RAPID COMMUNICATION

Mig, the Monokine Induced By Interferon-γ, Promotes Tumor Necrosis In Vivo

By Cecilia Sgadari, Joshua M. Farber, Anne L. Angiolillo, Fang Liao, Julie Teruya-Feldstein, Parris R. Burd, Lei Yao, Ghanshyam Gupta, Chiharu Kanegane, and Giovanna Tosato

Mig, the monokine induced by interferon-γ, is a CXC chemokine active as a chemoattractant for activated T cells. Mig is related functionally to interferon-inducible protein 10 (IP-10), with which it shares a receptor, CXCR3. Previously, IP-10 was found to have antitumor activity in vivo. In the present study, murine Mig RNA was found to be expressed at higher levels in regressing Burkitt's lymphoma tumors established in nude mice compared with progressively growing tumors. Daily inoculations of purified recombinant human Mig into Burkitt's tumors growing subcutaneously in nude mice consistently caused tumor necrosis associated with extensive vascular damage. These effects were indistinguishable from those produced by intratumor inoculations of Burkitt's tumors with IP-10. These results support the notion that Mig, like IP-10, has antitumor activity in vivo.

CHEMOKINES ARE A group of small secreted proteins that exert their effects through seven transmembrane-domain G-protein–coupled receptors and are active as chemotactic factors and regulators of cell growth.[1,2] With the exception of lymphotactin, chemokines contain four invariant cysteines, and are divided into the α (or CXC-) and β (or CC-) subgroups based on the presence or absence of an intervening amino acid between the first two of four conserved cysteines.

Mig, a chemokine of the CXC subfamily, was identified by differential screening of a cDNA library prepared from lymphokine-activated macrophages.[3] The Mig gene is expressed in monocytes/macrophages (unpublished data), hepatocytes, fibroblasts, keratinocytes, and endothelial cells in response to interferon-γ (IFN-γ).[3-5] In mice, systemic administration of IFN-γ and infection with protozoa or virus was associated with induction of the Mig gene in a variety of tissues, including liver, spleen, heart, and lung.[5] Functionally, Mig has been shown to target activated T cells, causing both an increase in $[Ca^{2+}]_i$ ions and chemotaxis.[6] Mig was also reported to inhibit angiogenesis in vivo.[7]

A comparison of chemokine protein sequences shows that human Mig is related to human interferon-inducible protein 10 (IP-10), with the chemokines sharing 37% amino acid identity over the portions of their sequence that are comparable.[8,9] The genes for human Mig and IP-10 were found to be adjacent on chromosome 4q21.21, suggesting a close evolutionary relationship.[10] Functionally, both Mig and IP-10 are chemotactic for activated T cells[6,11,12] and act as inhibitors of angiogenesis in vivo.[7,13-16] Additionally, IP-10, but not Mig, was reported to inhibit colony formation by hematopoietic cells[17] and to stimulate monocyte chemotaxis.[12] Human Mig and IP-10 showed reciprocal desensitization on human T cells, suggesting that they share a receptor.[6] This was recently confirmed with the cloning of a Mig/IP-10 receptor, CXCR3.[11] CXCR3 is highly expressed in activated but not resting T cells and mediates T-cell chemotaxis in response to Mig or IP-10 but not other chemokines.[11]

Recently, we have developed and characterized an experimental athymic murine system in which necrosis and regression of experimental Burkitt's lymphoma (BL) and other human malignancies are induced reproducibly by inoculation of Epstein-Barr virus (EBV)-immortalized human lymphocytes.[18,19] In an effort to understand the murine host response leading to tumor rejection, we analyzed patterns of murine cytokine/chemokine gene expression in response to Burkitt's tumors.[20] Using a semiquantitative reverse transcriptase-polymerase chain reaction (RT-PCR) analysis, we found the PCR products of IL-12p35, IFN-γ , RANTES, IP-10, and Mig to be more abundant from regressing tumors than from progressive tumors.[20] The PCR products of other chemokine genes, including JE, macrophage inflammatory protein-1α (MIP-1α), and MIP-1β, were detected at similar levels in both regressing and progressive tumors. When IP-10 was injected into Burkitt's tumors established in nude mice, it consistently caused tumor necrosis associated with vascular damage and intravascular thrombosis.[20] In addition, constitutive expression of murine IP-10 in Burkitt's cells reduced significantly their ability to grow as subcutaneous tumors in nude mice and caused tumor tissue necrosis. However, in contrast to treatment with EBV-immortalized B cells, IP-10 treatment never caused complete tumor regressions, raising the possibility that IP-10 might be one of a number of cytokines/chemokines involved in tumor regression in this model.[20]

In the present study, we sought to identify other factors that may contribute to Burkitt's tumor necrosis induced by EBV-immortalized cells in athymic mice.

MATERIALS AND METHODS

Cell lines and cell cultures. The human BL cell line CA46 was derived by spontaneous outgrowth of single-cell suspended human

From the Center for Biologics Evaluation and Research, Bethesda, MD; the Laboratory of Clinical Investigation, National Institute of Allergy and Infectious Diseases, National Institutes of Health, Bethesda, MD; the Department of Hematology/Oncology, Children's National Medical Center, Washington, DC; and the Laboratory of Pathology, Hematopathology Section, National Cancer Institutes, Bethesda, MD.

Submitted December 23, 1996; accepted January 27, 1997.

Address reprint requests to Giovanna Tosato, MD, Division of Hematologic Products, Center for Biologics Evaluation and Research, Bldg 29A, Room 2D16, HFM-535, 8800 Rockville Pike, Bethesda, MD 20892.

The publication costs of this article were defrayed in part by page charge payment. This article must therefore be hereby marked ''advertisement'' *in accordance with 18 U.S.C. section 1734 solely to indicate this fact.*

0006-4971/97/8908-0051$0.00/0

BL tissue.[21] The EBV-immortalized VDS-O cell line was obtained by spontaneous outgrowth of peripheral blood B cells from an EBV-seropositive normal individual.[22] All cell lines were maintained in RPMI 1640 medium (Biofluids, Rockville, MD) supplemented with 10% heat-inactivated fetal bovine serum (FBS; Intergen Co, Purchase, NY), 2 mmol/L L-glutamine (GIBCO BRL, Grand Island, NY), and 5 μg/mL gentamicin (Sigma, Chemical Co, St Louis, MO). All cell lines were mycoplasma-free.

Animal studies. Six-week-old BALB/c nu/nu mice were obtained from the National Cancer Institute (National Institute of Health [NIH], Frederick, MD) and maintained in pathogen-limited conditions. The mice received 400 rad total body irradiation and 24 hours later were injected subcutaneously in the right abdominal quadrant with 10^7 exponentially growing CA46 BL cells in 0.2 mL RPMI 1640 medium supplemented with 10% FBS.[18] All animals were observed twice weekly, and tumor size was estimated (in square centimeters) as the product of two-dimensional caliper measurements (longest perpendicular length and width). Regression of Burkitt's tumors was achieved by weekly inoculation of established tumors (measuring at least 0.2 cm^2) with 10^7 EBV-immortalized VDS-O cells in 0.2 mL RPMI 1640 medium containing 10% FBS.[18] Test mice bearing established Burkitt's tumors (at least 0.15 cm^2 in size) were injected daily into the tumor (for 30 to 43 days) with human rMig or human rIP-10, both at 400 ng dose, or with appropriate formulation buffer control (injection volume, 0.2 mL). The human Mig protein was the mature, 103 amino acid recombinant protein purified from an overexpressing Chinese hamster ovary (CHO) cell line.[6] The expression and purification of Mig is described below. As a source of human IP-10, we used recombinant purified (>90% pure as evaluated by silver staining) human IP-10 from PeproTech Inc (Rocky Hill, NJ). The formulation buffer used to dilute IP-10 and Mig consisted of saline solution containing 50 mg/mL human serum albumin and 5 mg/mL mannitol. The same formulation buffer was used in control injections. The care and use of mice was in accordance with the NIH guidelines on animal care.

Expression of human rMig in CHO cells. Transfection of human Mig into CHO cells was performed as described.[6] Briefly, a 785-bp fragment containing the entire coding sequence of human Mig was inserted into the vector pMSXND downstream the metallothionein 1 promoter; the vector also contained a neomycin resistance gene and cDNA sequence for mouse dihydrofolate reductase. pMSXND-Mig was linearized and transfected into CHO cells by the lipofectin method (GIBCO BRL). Transfected cells were selected in 400 μg/mL G418 (GIBCO BRL), followed by culture without G418 but with 0.2 μmol/L methotrexate (Sigma Chemical Co) in minimum essential medium-α (MEM-α) supplemented with 11.5 μg/mL proline and 10% dialyzed fetal calf serum (Sigma Chemical Co). Methotrexate-resistant colonies were analyzed for production of human Mig by sodium dodecyl sulfate-polyacrylamide gel electrophoresis followed by immunoblotting. The CHO/H9 line was chosen for human Mig production. For collecting supernatants for protein purification, human rMig-overexpressing CHO cells were cultured in MEM-α supplemented with 10% dialyzed fetal calf serum, 0.2 μmol/L methotrexate, and 2 mmol/L glutamine (Sigma Chemical Co) until confluent. The medium was then discarded and replaced with serum free MEM-α containing 100 mmol/L cadmium sulfate (Sigma Chemical Co). The serum-free MEM-α media was changed every 24 hours through day 7, and the supernates collected from day 2 to 7 were used as starting material for protein purification.

Purification of human rMig. Purification of human rMig was performed essentially as described.[6] Briefly, human rMig-containing supernates were equilibrated into 50 mmol/L Tris/HCl, pH 7.5, and 0.5 mmol/L EDTA. Supernatants (8 to 10 L) were loaded on carboxymethyl (CM)-cellulose column (MetaChem Technologies Inc, Torrance, CA) mounted on a ConSep liquid chromatograph (Millipore Co, Milford, MA), and the bound protein was eluted with a linear gradient of 0.025 to 1 mol/L NaCl in 50 mmol/L Tris/HCl, pH 7.5, 0.5 mmol/L EDTA. The full-length secreted protein eluted as a single asymmetrical peak at 7E0.5 mol/L NaCl. Fractions containing rMig were identified by immunoblotting; pooled peak fractions were concentrated by a Centriprep-3 device (Amicon Inc, Beverly, MA) and subjected to reversed-phase high-performance liquid chromatography (HPLC) on a C18 column (Vydac, Hesperia, CA). rMig was eluted using a gradient of 15% to 40% acetronile in 0.05% TFA over 60 minutes at a flow rate of 1 mL/min on a liquid chromatograph (model 1050; Hewlett-Packard Co, Palo Alto, CA). The column eluate was monitored at 280 nm, 205 nm, and, for reference, at 450 nm. The full-length rMig eluted at 44 minutes. HPLC fractions with purified human rMig were evaporated to dryness, and the protein was resuspended in 10 mmol/L Tris/HCl, pH 7.5, and stored at −70°C. rMig concentration was determined by the bicinchoninic acid method according to the manufacturer's protocol (Pierce Chemical Co, Rockfield, IL), using bovine serum albumin as standard. The homogeneity of purified Mig was determined by silver staining and Mig identity was verified by immunoblotting, as described.[6] The biologic activity of purified Mig was confirmed by calcium flux assays using activated T cells, as described.[6]

RT-PCR analysis. Total cellular RNA was isolated from tumors by guanidine thiocyanate/CsCl centrifugation, and 4 μg aliquots were reverse transcribed using an Rnase H^- RT (Superscript; GIBCO/BRL). Eighty nanograms of the resultant cDNA was amplified using radiolabeled dNTP by a semiquantitative PCR.[23] The number of amplification cycles was selected for each primer pair to provide the maximum signal intensity within the linear portion of a product versus template amplification curve.[23] Aliquots from each amplification reaction were electrophoresed on 6% acrylamide (Long Ranger; AT Biochem, Malvern, PA) Tris-borate EDTA gels, followed by autoradiography and quantification by phosphorimage analysis. Nucleotide sequences for murine 5′ and 3′ primers, respectively (followed in parenthesis by annealing temperature in degrees celsius), were as follows: IP-10, ACCATGAACCCAAGTGCTGCCGTC and GCTTCACTCCAGTTAAGGAGCCCT (64); IFN-γ, TGCGGCCTAGCTCTGAGACAATGA and TGAATGCTTGGCGCTGGACCTGTG (64); IL-12 (p35), TCCAGCATGTGTCAATCACGCTAC and GTTGATGGCCTGGAACTCTGTCTG (62); IL-12 (p40), CCGGTTTCCATCGTTTTGCTGG and AGAGTCAGGGGAACTGCTACTGCT (56.5); Mig, ACTCAGCTCTGCCATGAAGTCCGC and AAAGGCTGCTCTGCCAGGGAAGGC (66); G3PDH, GCCACCCGAAAGACTGTGGATGGC and CATGTAGGCCATGAGGTCCACCAC (56.5); tumor necrosis factor α (TNFα), CACAGAAAGCATGATCCGCG and GGCACCACTAGTTGGTTGTC (59); IL-6, ATGAAGTTCCTCTCTGCAAGAGACT and CACTAGGTTTGCCGAGTAGATCTC (59). The number of amplification cycles used were 21 for G3PDH; 26 for IP-10; 27 for Mig; 30 for IL-6, IFN-γ, and IL-12 p35 subunit; and 31 for TNFα and IL-12 p40 subunit. Primers were designed to discriminate between genomic and cDNA by spanning at least one intron/exon boundary.

Northern blot analysis. Total cellular RNA was extracted from tumor tissues by guanidine thiocyanate/CsCl centrifugation, and 20 μg of each RNA sample was separated through MOPS-formaldehyde 1% agarose gels and transferred to nylon membranes (GIBCO BRL). The filters were hybridized under standard conditions to gel-purified cDNA probes labeled with ^{32}PdCTP by the random primer method (Amersham Corp, Arlington Heights, IL). The cDNAs used as G3PDH and murine Mig probes were previously described.[5] Bands were quantified using a Molecular Dynamics Phosphorimager (Sunnyvale, CA) and normalized to the levels of G3PDH.

Histology. Tumors were removed in toto, fixed in 10% neutral buffered formalin solution (Sigma), embedded in paraffin, sectioned

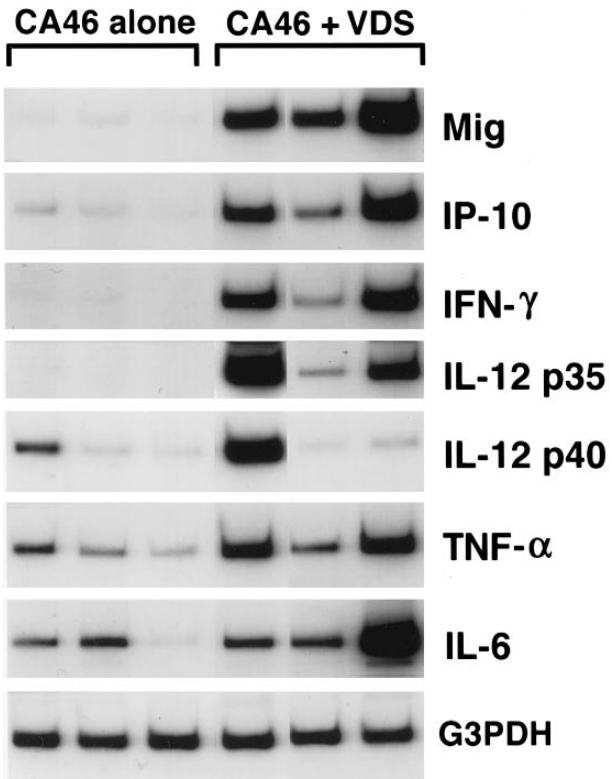

Fig 1. Cytokine and chemokine mRNAs in regressing and progressive Burkitt's tumors shown by semiquantitative RT-PCR analysis. Tissue fragments were obtained from regressing and progressive Burkitt's tumors established in BALB/c nu/nu mice by subcutaneous inoculation of 10^7 BL cells (CA46 cell line). Tumor regression was induced by weekly intratumor inoculation of 10^7 LCL (VDS cell line), as described. Regressing tumors were harvested when LCL-treated Burkitt's tumors developed typical tumor necrosis and scarring, lesions that are indicative of an effective antitumor response. Progressive tumors were harvested from untreated Burkitt's tumors. Total cellular RNA, isolated from tumor tissues, was subjected to RT-PCR analysis.

at 4 μm, and stained with hematoxylin and eosin or elastin van Gieson (EVG) reagent.

Statistical analysis. A Student's *t*-test and Dunnett's method were used to evaluate the significance of group differences.

RESULTS

Mig expression in BL established in athymic mice. Preliminary experiments using RT-PCR analysis suggested that Burkitt's tumors undergoing regression in athymic mice expressed higher levels of Mig mRNAs compared with progressively growing tumors.[20] We wished to examine further the patterns of expression of the murine Mig gene in experimental Burkitt's tumors. To this end, Burkitt's tumors were established in 14 athymic mice by subcutaneous inoculation with 10^7 CA-46 cells. Tumor regression was induced in 7 mice by weekly intratumor inoculations with 10^7 lymphoblastoid cells (LCL; VDS-O cell line). Tumors were removed from the LCL-treated mice after developing typical tumor necrosis and scarring, lesions that are indicative of an effective antitumor response. Progressive Burkitt's tumors were harvested in parallel from untreated mice. Using a semiquantitative RT-PCR method for analysis of 6 of the tumor specimens (Fig 1), we found the PCR products for murine Mig to be consistently more abundant in the regressing than in the progressive tumors studied. The PCR products for murine IP-10, IFN-γ,, IL-12 p35 subunit, and IL-6 were also found to be more abundant in the regressing than in the progressive tumors studied, whereas those for murine IL-12 p40 subunit and TNFα were detected at variable levels in these groups (Fig 1). Northern blot analysis performed with RNAs extracted from the remaining 8 tumors confirmed that murine Mig mRNA was expressed at significantly higher levels in 4 regressing Burkitt's tumors compared with 4 progressive Burkitt's tumors (Fig 2). Expression of human Mig was undetectable by RT-PCR in the Burkitt's CA-46 and the LCL VDS lines (data not shown).

Mig treatment of BL in athymic mice. Full-length Mig protein was purified to a high degree of homogeneity from culture supernatants of CHO cells overexpressing recombinant human Mig, and its identity was confirmed by immunoblotting with a rabbit antihuman Mig serum.[6] Purified human rMig was injected daily for 30 to 40 days at the dose of 400 ng into Burkitt's tumors established subcutaneously in athymic mice ($\geq$0.3 cm^2 in size), and its effects were compared with those from intratumor inoculations with human rIP-10 (400 ng/mL daily) or LCL (10^7 cells weekly; Table 1). As expected, tumors injected with LCL or with IP-10 developed a visible response to treatment characterized by superficial necrosis and scarring that progressively extended to encompass variable portions of the visible tumor. Mig-treated tumors also developed visible necrosis and scarring that were indistinguishable in appearance from those exhibited by IP-10–treated mice. These lesions appeared after an average of 29 (range, 24 to 35) injections with Mig as opposed to 26 (range, 21 top 29) injections with IP-10. In no case did Mig treatment cause complete tumor regressions or halt tumor growth, as measured by caliper (Table 1). However, when removed in toto and sectioned at the completion of treatment, Mig-treated tumors were found to be 41% necrotic (Table 1). Previously, we noted that treat-

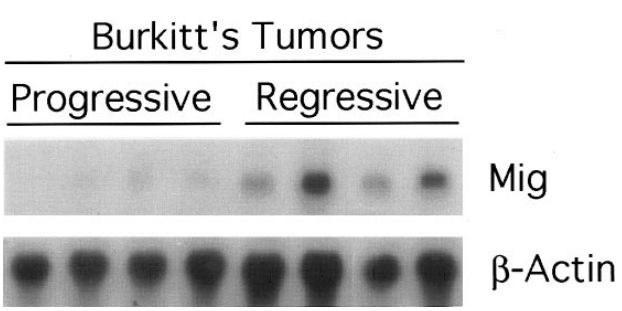

Fig 2. Expression of murine Mig mRNA in progressive and regressing Burkitt's tumors assessed by Northern blot analysis. Total RNA was extracted from tissue fragments of progressively growing or regressing Burkitt's tumors induced as desribed in the legend to Fig 1, separated on a 1.2% agarose gel, transferred to nitrocellulose membrane, and hybridized for murine Mig and G3PDH.

Table 1. Effects of Human rMig Treatment on Burkitt's Tumor in Athymic Mice

Treatment	Mice Treated	Day of First Injection (±SD)*	Tumor Size at First Injection (±SD)†	Total Days of Treatment (±SD)	Tumor Size at End of Treatment (±SD)†	% Tumor Necrosis (±SD)‡	% Damaged Vessels (±SD)§
None	3	—	—	—	8.06 (3.1)	11.5 (6.2)	56.6 (9.8)
LCL	2	22	0.33	33.0	5.93	44.75	66.0
Buffer	4	13.2 (2.2)	0.24 (0.1)	35.0 (1.7)	10.6 (1.1)	25.3 (7)	48.6 (15)
rMig	4	13.7 (1.6)	0.34 (0.02)	39.0 (5.3)	9.9 (0.5)	40.6 (10.7)	76.5 (4.1)
rIP-10	4	13.7 (1.8)	0.23 (0.1)	38.2 (5.3)	8.3 (2.4)	39.8 (10.8)	78.3 (2)

Nude mice bearing a Burkitt's tumor (CA46 line) induced as described in the Materials and Methods were injected daily into the tumor with human rMig or human rIP-10 at the dose of 400 ng (in 0.2 mL of a formulation buffer containing 50 mg/mL human serum albumin) for 30 to 43 days. Tumor-bearing control animals were injected into the tumor either with LCL (10^7 VDS cells/week in 0.2 mL normal saline) or with formulation buffer (0.2 mL daily).

* Calculated from day of Burkitt's cell line injection; expressed as arithmetic mean for the group (±SD).

† Calculated as the product of two-dimensional caliper measurement (longest perpendicular length and width); expressed in square centimeter as arithmetic mean for the group (±SD).

‡ The percentage of tumor tissue necrosis was estimated by digital analysis of tumor cross-sections corresponding to the largest portion of the tumor. The slides were scanned using a flat bed scanner (Scanjet II CX; Hewlett Packard) and necrotic/total tumor area was measured; expressed as arithmetic mean for the group (±SD).

§ Tumor sections were stained with EVG reagent and vessels staining at least in part with EVG were evaluated for vascular damage consisting of elastin fiber fragmentation and disruption with or without associated tumor infiltration, fibrinoid necrosis, or fibrin thrombi. The results are expressed as mean (±SD) percentage of damaged vessels estimated after evaluation of all EVG staining vessels in the tumor sections.

ment with IP-10 produced only incomplete tumor regressions in the same tumor model used here and had no effect on visible tumor growth evaluated by caliper,[20] a result confirmed here. In the present experiments, IP-10–treated tumors were found to be 40% necrotic, whereas untreated and buffer treated tumors were found to be only 12% and 25% necrotic, respectively (Table 1). The differences in the extent of tumor necrosis in Mig or IP-10–treated tumors compared with controls (untreated and buffer-treated) tumors are significant ($P = .011$ and .014, respectively by Student's *t*-test), indicating that Mig and IP-10 caused a reduction of viable tumor tissue.

Histologically, Mig-treated tumors generally displayed central and homogeneous tissue necrosis extending to the epidermis and deep into the tumor mass (Fig 3J and K). The boundaries between necrotic and viable tumor tissue were abrupt, and infiltration with lymphocytes, neutrophils, and monocytes was not signicantly different from that observed in control animals. Within the viable tumor tissue, both distant and proximal to the necrotic tumor tissue, there was evidence of vessel injury characterized by intimal thickening and intraluminal thrombosis (Fig 3L). The histologic appearance of IP-10–treated tumors was indistinguishable from that of Mig-treated tumors (Fig 3M, N, and O). In contrast, control Burkitt's tumors, either untreated (Fig 3A, B, and C) or treated with buffer alone (Fig 3G, H, and I), displayed little or no tumor tissue necrosis.

To estimate the extent of vascular damage, one tumor section from each of the tumors was stained with EVG reagent, which is specific for elastin fibers in the external and internal elastic lamina of muscular arteries and the internal elastic lamina of large arterioles. Normal elastin laminas from these tumors appear continuous, regularly folded, and uniformly thick (Fig 4A and B). In contrast, damaged elastin laminas appear fragmented, irregular in thickness, or flat, and these abnormalities are often associated with intravascular thrombosis, fibrinoid necrosis, or tumor infiltration (Fig 4C and D). All vessels that stained, at least in part, with EVG were evaluated, thereby excluding nonviable vessels, capillaries, and adventitial vasa vasorum. Sections from untreated

Fig 3. Gross and microscopic morphology of progressive and regressing BL tumors. Female BALB/c nu/nu 6- to 8-week-old mice were injected subcutaneously with 10^7 BL cells. After tumor development, mice were observed or injected into the tumor with either LCL, human rMig, or human rIP-10. Tumors were removed in toto 5 to 6 weeks after the initial inoculation and processed for histology. (A through C) Tumor tissue from a mouse injected subcutaneously with CA46 Burkitt's cells. (D through F) Tissue from a tumor induced by subcutaneous injection with CA46 Burkitt's cells and subsequently injected with LCL (VDS line) weekly for 3 weeks. (G through I) Tissue from a tumor induced by subcutaneous injection with CA46 Burkitt's cells and subsequently injected daily with formulation buffer (0.2 mL into the tumor). (J through L) Tissue from a tumor induced by subcutaneous injection with CA46 Burkitt's cells and subsequently injected daily with human rMig (400 ng/d into the tumor). (M through O) Tissue from a tumor induced by subcutaneous injection with CA46 Burkitt's cells and subsequently injected daily with human IP-10 (400 ng/d into the tumor). (A, D, G, J, and M) Gross morphology of Burkitt's tumors removed in toto with abstract epidermidis and dermis showing in (A) and (G) mostly viable looking tumor tissue with small and patchy areas of necrosis and in (D), (J), and (M) regressing tumors with extensive central necrosis surrounded by viable tumor (no magnification). (B, E, H, K, and N) Microscopic morphology (original magnification ×5) of Burkitt's tumors extending to the epidermidis; in (B) and (H) viable-looking tumor tissue; and in (E), (K), and (N) the abrupt interface between necrotic and viable tumor tissue. (C, F, I, L, and O) Higher power magnification (×20) of viable tumor tissue with patent capillaries (containing red blood cells) in (C) and (I) and capillaries occluded with thrombi at various stages of reorganization in (F), (L), and (O).

and buffer-treated tumors displayed evidence of vascular damage in 56.6% and 48.5% of EVG-staining vessels, respectively, as opposed to 76.5% and 78.3% of EVG-staining vessels in Mig- and IP-10–treated tumors, respectively (Table 1). Thus, vascular damage was common in all tumors, but occurred at a greater frequency in Mig- and IP-10–treated tumors compared with untreated or buffer-treated tumors (the difference was significant at the .05 level by Dunnett's method).

We examined the patterns of cyto/chemokine gene expression in Mig-treated tumors and compared it with those of control and IP-10–treated tumors by semiquantitative RT-PCR analysis. The results from two representative Mig-, IP-10–, and control-treated tumors are shown

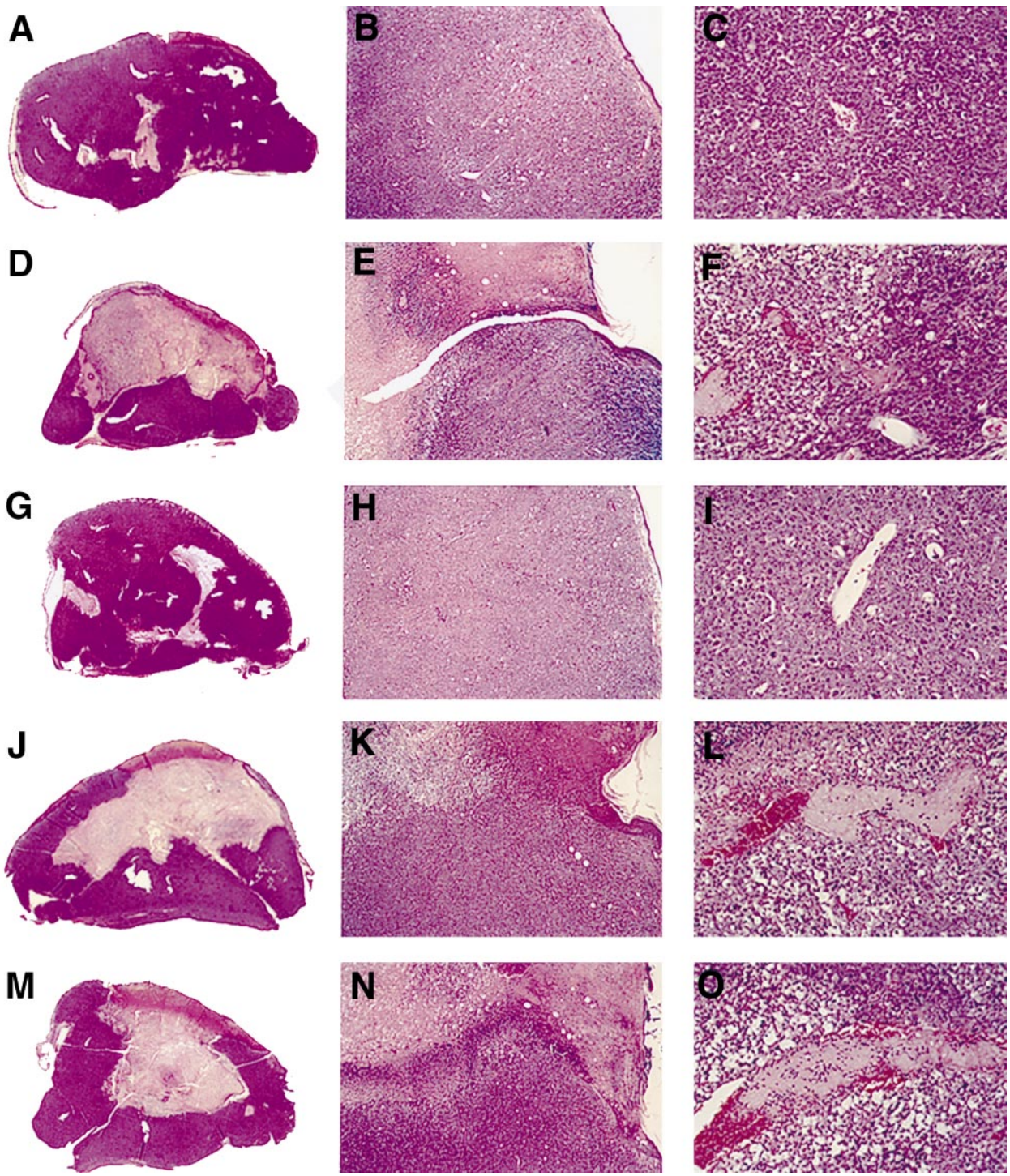

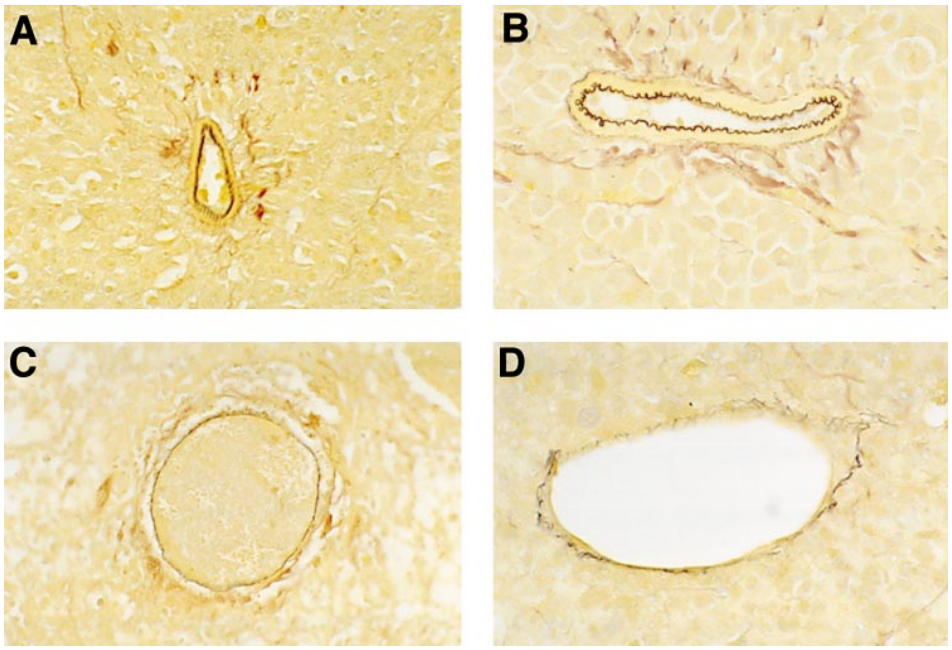

Fig 4. Microscopic morphology of BL vessels evaluated by staining with EVG reagent that is specific for elastin fibers in the external and internal elastic lamina of muscular arteries and the internal elastin lamina of large arterioles. Elastin fibers stain dark brown with EVG reagent. (A and B) Normal appearing patent vessels with continuous and regularly folded elastin laminas in tumor tissue from a mouse treated with formulation buffer. (C and D) Damaged vessels with fragmented or flattened elastin laminas associated with intravascular thrombosis in tumor tissue from a mouse bearing a regressing Burkitt's tumor treated with human rMig. (A and C), original magnification ×40; (B and D), original magnification ×63.

in Fig 5. The PCR products for murine Mig, IP-10, IFN-γ, IL-12 p35 and p40 subunits, TNFα, and IL-6 were detected at variable levels in tumor tissues from all tumor samples, and these levels appeared unrelated to the extent of tumor necrosis exhibited by these tissues.

DISCUSSION

In this study we show that Mig treatment of subcutaneous Burkitt's tumors in nude mice promotes tumor tissue necrosis. Histologically, Mig-treated tumors displayed a deep central necrosis involving, on the average, 40.6% of the tumor mass and was sharply separated from the surrounding live tumor tissue. The inflammatory infiltration was not prominent and did not differ from that observed in control treated mice. Vascular damage, evidenced by elastin disruption and intravascular thrombosis, was extensive and widespread throughout the tumor, including the surrounding viable tumor tissue. This morphology closely resembles that displayed by IP-10 or LCL-treated Burkitt's tumors, with the notable exception of monocyte/macrophage infiltration that is characteristic of LCL-treated, but not Mig- or IP-10–treated, tumors. A likely consequence of this difference in the extent of monocyte infiltration is the increased expression of a variety of cyto/chemokines, including TNFα, IP-10, and Mig, in LCL-treated but not Mig- or IP-10–treated, tumors.

Biologic properties previously attributed to Mig include chemoattraction of activated T cells,[6] inhibition of endothelial cell chemotaxis,[7] and inhibition of growth factor-induced angiogenesis in vivo.[7] Human Mig and IP-10 showed reciprocal desensitization on human T cells, consistent with their sharing a receptor,[6] and this was confirmed recently with the identification of CXCR3.[11] These findings raise the possibility that other biologic properties presently attributed to IP-10 may also apply to Mig. In addition to functions known to be shared with Mig, IP-10 was reported to promote chemotaxis of natural killer (NK) cells and monocytes, to promote T-cell adhesion to endothelial cells, to inhibit colony formation by human hematopoietic cells, and to stimulate NK cell cytolysis. Because the recently described Mig/IP-10 receptor is expressed on activated T and NK cells, but not on monocytes, B cells, resting T cells, neutrophils, or other cell types,[11] it is presently unclear whether all biologic functions attributed to IP-10 are a consequence of signalling through the Mig/IP-10 receptor, whether other receptors may exist, or whether, for example, the monocyte chemoattractant activity attributed to IP-10 was artifactual. Mig and IP-10 appear not to share receptors with other chemokines.[2] Heparinase-sensitive binding sites for IP-10 have been detected on a variety of cell types, including endothelial, epithelial, and hematopoietic cells, and these may contribute to chemokine binding to the cell surface.[15] Whether Mig and IP-10 bind to similar heparan sulfate proteoglycans is unknown.

IP-10 was reported to exibit antitumor effects in distinct preclinical models.[20,24,25] In one setting,[24] murine plasmacytoma and breast adenocarcinoma cell lines genetically engineered to secrete high levels of murine IP-10 were found to elicit a potent antitumor effect in normal mice, resulting in their failure to develop tumors. This effect of IP-10 was considered T-cell–dependent because it was not reproduced in athymic mice and in euthymic mice was accompanied by the induction of a brisk inflammatory response with lymphocytes, neutrophils, and monocytes.[24] In another model,[25] intratumor inoculation of IP-10 into human adenocarcinoma established subcutaneously in SCID mice caused a reduction of tumor size and of the number of lung metastasis. IP-10 did not stimulate neutrophil and macrophage infiltration of the tumors and appeared to exert its antitumor effect indepen-

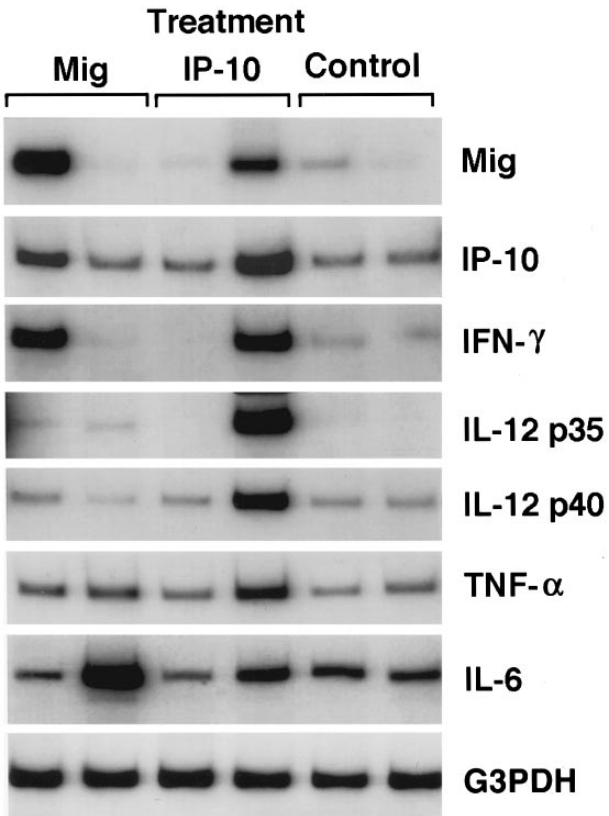

Fig 5. Representative patterns of cytokine and chemokine mRNA expression in Mig-, IP-10–, or buffer-treated Burkitt's tumors shown by semiquantitative RT-PCR analysis. Total cellular RNA was extracted from Burkitt (CA46 cell line) tumors established in athymic mice and subsequently treated with intratumor inoculations of either human rMig (400 ng/d), human rIP-10 (400 ng/d), or diluent (0.2 mL/d), as described in the legend to Table 1.

dently of T- and B-cell immunity because its effects were observed in SCID mice. Because a correlation was found between the antitumor effects of IP-10 and the reduction in tumor vascularization, it was proposed that the angiostatic effect of IP-10 was responsible for its antitumor effects.[25] In a nude mouse model,[20] we found that inoculation of IP-10 into subcutaneously established BL caused tumor necrosis and widespread vascular damage, but no appreciable inflammatory response with neutrophils, monocytes, or lymphocytes. In the same athymic mouse model, expression of IP-10 into Burkitt's cells resulted in reduced tumor growth and extensive tumor necrosis associated with vascular damage.[20] We concluded that the antitumor effects of IP-10 were likely a consequence of an effect on tumor vasculature, including an angiostatic effect limiting tumor neovascularization and a damaging effect on established tumor vasculature.[20]

The antitumor effects of IP-10 in distinct experimental tumor models have previously been linked to a chemokine effect either on T cells or endothelial cells.[20,24,25] Using one of these tumor models,[20] we show here that Mig exhibits antitumor effects that are indistinguishable from those of IP-10. Both because the experiments were performed in young athymic mice that had few circulating T cells and because Mig-treated tumors showed little or no increase in lymphoid infiltrates compared with controls, we believe that T cells are unlikely mediators of the antitumor effects of Mig. Rather, all the evidence points towards a vascular-based effect. Mig-treated tumors displayed central and homogeneous necrosis, as one might expect from insufficient tumor blood perfusion, and generalized evidence of vascular damage associated with elastin destruction and intravascular thrombosis. Previously, Mig was reported to reduce endothelial cell chemotaxis in vitro,[7] suggesting that it can target endothelial cells directly. In vivo, Mig was reported to inhibit neovascularization induced by the angiogenic factors IL-8, ENA-78, GCP-2, and GROα.[7] Although these previously described properties of Mig indicate that the chemokine can target blood vessels, the antitumor effects of Mig described here cannot be explained simply on the basis of its angiostatic effects. Diminished tumor growth due to reduced tumor vascularization would be expected, but injury to established tumor vasculature has not generally characterized the effects of other inhibitors of angiogenesis, except IP-10.

The potential role of NK cells in mediating the antitumor effects of Mig was considered. We found no evidence of increased numbers of NK cells or increased NK cell function in the spleens of IP-10[20] or Mig-treated animals (not shown), and, as mentioned above, we found no prominent lymphoid infiltration in LCL-, IP-10–, or Mig-treated tumors. Also, expression of the murine IFN-γ and TNFα genes appeared not to be consistently increased in Mig-treated tumors compared with controls, because an increase might be expected if NK cells were involved in tumor cytolysis.[26] Nonetheless, NK cells are capable of lysing tumor cells, and, occasionally, IL-2–activated NK cells have induced clear antitumor responses in vivo.[26-28] In addition, NK cells express the IP-10/Mig receptor,[11] and one might expect Mig, like IP-10, to be chemotactic for activated NK cells. Furthermore, we know that activated NK cells can undergo rapid apoptotic cell death after engagement in target cell lysis.[29] If so, NK cells may be difficult to detect at the tumor site, but nonetheless be effective mediators of tumor cell death.

Unlike LCL-treatment of BL in nude mice that often causes complete tumor regressions and cures,[18] Mig- or IP-10–treated tumors showed only partial responses. In no cases were Mig or IP-10 treatments curative in the present tumor model. However, both because the mRNAs for these chemokines were significantly induced in Burkitt's tumors treated with LCL, and, because IP-10 and Mig injected individually into established Burkitt's tumors exhibited clear antitumor effects, we believe that both these chemokines participate in tumor regression induced by LCL. It is possible that insufficient chemokine levels were achieved at the tumor site by intratumor inoculation of IP-10 or Mig or that other cytokines/chemokines, also induced during LCL treatment, might be involved in tumor regression in this system. It is also possible that Mig might act additively or synergistically with IP-10 in promoting tumor regression.

One of the important issues raised by this possibility and, in general, by the existence of cytokines/chemokines with

overlapping biologic activities, is the reason for such redundancy. It could be that production of these chemokines occurs in different cell types and tissues and is regulated by distinct mechanisms. We did not examine the cellular sites of production of IP-10 and Mig within regressing tumors, and, although we find evidence of increased IFN-γ expression within regressing tumors, we do not know whether IFN-γ represents the only inducer in this system. Recently, it was reported that, during acute infection with either Plasmodium yoeli, Toxoplasma gondii, or vaccinia virus, the liver was always the site of greatest expression of the Mig gene, whereas expression of IP-10 was more variable among the various organs.[5] In addition, although induction of Mig during infections required the expression of IFN-γ, induction of IP-10 was not completely dependent on IFN-γ.[5] Another possibility is that redundancy of certain biologic functions might coexist with unique functions. Recently, it was reported that the pituitary adenylyl cyclase-activating polypeptide (PAPCAP) receptor can be differentially coupled to two transduction pathways through distinct ligands.[30] In this setting, depending on the fine molecular interactions within the binding site, IP-10 and Mig may induce distinct signals and produce distinct biologic effects. Alternatively, unique functions could derive from the coexistence of a shared CXCR3 receptor with unique receptors.

We report here that Mig has antitumor activity in vivo, a previously unrecognized biologic property of this chemokine. Because of their more restricted spectrum of activities, chemokines such as Mig and IP-10 may provide therapeutic tools that are more selective than those provided by pleiotropic cytokines such as IFN-γ, TNFα, IL-1α, IL-6, and IL-12 that have the potential for producing a multitude of biologic effects. It may also lead to the development of better anticancer therapies, particularly in the context of T-cell immunodeficiency.

ACKNOWLEDGMENT

We thank the animal facility personnel; Drs Elaine Jaffe, Amy Rosenberg, and Barbara Ensoli for their suggestions; Dr Dennis Taub for providing human rIP-10; and Dr Hirokazu Kanegane for help.

REFERENCES

1. Miller MD, Krangel MS: Biology and biochemistry of the chemokines: A family of chemotactic and inflammatory cytokines. Crit Rev Immunol 12:17, 1992

2. Mackay CR: Chemokine receptors and T cell chemotaxis. J Exp Med 184:799, 1996

3. Farber J: A macrophage mRNA selectively induced by gamma-interferon encodes a member of the platelet factor 4 family of cytokines. Proc Natl Acad USA 87:5238, 1990

4. Farber JM: HuMIG: A new human member of the chemokine family of cytokines. Biochem Biophys Res Commun 192:223, 1993

5. Amichay D, Gazzinelli RT, Karupiah G, Moench TR, Sher A, Farber JM: The genes for chemokines MuMig and Crg-2 are induced in protozoan and viral infections in response to IFN-g with patterns of tissue expression that suggest non-redundant roles in vivo. J Immunol 157:4511, 1996

6. Liao F, Rabin R, Yannelli J, Koniaris L, Vanguri P, Farber J: The human Mig chemokine: Biochemical and functional characterization. J Exp Med 182:1301, 1995

7. Strieter RM, Polverini PJ, Arenberg DA, Kunkel SK: The role of CXC chemokines as regulators of angiogenesis. Shock 4:155, 1995

8. Luster A, Unkeless J, Ravetch J: γ-Interferon transcriptionally regulates an early response gene containing homolgy to platelet proteins. Nature 315:672, 1985

9. Luster A, Ravetch J: Biochemical characterization of a γ interferon-inducible cytokine (IP-10). J Exp Med 166:1084, 1987

10. Lee H-H, Farber JM: Localization of the gene for the human MIG cytokine on chromosome 4q21 adjacent to INP10 reveals a chemokine ''mini-cluster''. Cytogenet Cell Genet 74:255, 1996

11. Loetscher ML, Gerber B, Loetscher P, Jones SA, Piali L, Clark-Lewis I, Baggiolini M, Moser B: Chemokine receptor specific for IP-10 and Mig: Structure, function and expression in activated T lymphocytes. J Exp Med 184:963, 1996

12. Taub D, Lloyd A, Conlon K, Wang J, Ortaldo J, Harada A, Matsushima K, Kelvin D, Oppenheim J: Recombinant human interferon-inducible protein 10 is a chemoattractant for human monocytes and T lymphocytes and promotes T cell adhesion to endothelial cells. J Exp Med 177:1809, 1993

13. Angiolillo A, Sgadari C, Taub D, Liao F, Farber J, Maheshwari S, Kleinman H, Reaman G, Tosato G: Human interferon-inducible protein 10 is a potent inhibitor of angiogenesis in vivo. J Exp Med 182:155, 1995

14. Sgadari C, Angiolillo A, Tosato G: Inhibition of angiogenesis by interleukin-12 mediated by the interferon-inducible protein 10. Blood 87:3877, 1996

15. Luster A, Greenberg S, Leder P: The IP-10 chemokine binds to a specific cell surface heparan sulfate site shared with platelet factor 4 and inhibits endothelial cell proliferation. J Exp Med 182:219, 1995

16. Strieter R, Kunkle S, Arenberg D, Burdick M, Polverini P: Interferon γ-inducible protein 10 (IP10), a member of the C-X-C chemokine family, is an inhibitor of angiogenesis. Biochem Biophys Res Commum 210:51, 1995

17. Sarris A, Broxmeyer H, Wirthmueller U, Karasavvas N, Cooper S, Lu L, Krueger J, Ravetch J: Human interferon-inducible protein 10: Expression and purification of recombinant protein demonstrate inhibition of early human hematopoietic progenitors. J Exp Med 178:1127, 1993

18. Tosato G, Sgadari C, Taga K, Jones KD, Pike SE, Rosenberg A, Sechler JMG, Magrath IT, Love LA, Bathia K: Regression of experimental Burkitt's lymphoma induced by Epstein Barr virus-immortalized human B cells. Blood 83:776, 1994

19. Angiolillo A, Sgadari C, Sheikh N, Reaman G, Tosato G: Regression of experimental human leukemias and solid tumors induced by Epstein-Barr virus immortalized B cells. Leuk Lymphoma 19:267, 1995

20. Sgadari C, Angiolillo AL, Cherney BW, Pike SE, Koniaris LK, Vanguri P, Burd PR, Sheikh N, Gupta G, Teruya-Feldstein J, Tosato G: Interferon-inducible protein-10 identified as a mediator of tumor necrosis in vivo. Proc Natl Acad Sci USA 93:13791, 1996

21. Shiramizu B, Barriga F, Neequaye J, Jafri A, Dalla-Favera R: Patterns of chromosomal breakpoint locations in Burkitt's lymphoma. Relevance to geography and Epstein-Barr virus association. Blood 77:1516, 1991

22. Tosato G, Blaese R, Yarchoan R: Relationship between immunoglobin production and immortalization by Epstein-Barr virus. J Immunol 135:959, 1985

23. Burd P, Thompson W, Max E, Mills F: Activated mast cells produce interleukin 13. J Exp Med 181:1373, 1995

24. Luster A, Leder P: IP-10, a -C-X-C- chemokine, elicits a potent thymus dependent antitumor response in vivo. J Exp Med 178:1057, 1993

25. Arenberg DA, Kunkel SL, Polverini PJ, Morris SM, Burdick

MD, Glass MC, Taub DT, Iannettoni MD, Whyte RI, Strieter RM: Interferon-γ-inducible protein 10 (IP-10) is an angiostatic factor that inhibits human non-small cell lung cancer (NSCLC) tumorigenesis and spontaneous metastasis. J Exp Med 184:981, 1996

26. Berke G: The function and mechanism of action of cytolytic lymphocytes, in Paul WE (ed): Fundamental Immunology (ed 3). New York, NY, Raven, 1993, p 965

27. Rosenberg S: Adoptive immunotherapy for cancer. Sci Am 262:62, 1990

28. Parmiani G: An explanation of the variable clinical response to interleukin-2 and LAK cells. Immunol Today 11:113, 1990

29. Taga K, Yamauchi A, Kabashima K, Bloom E, Muller J, Tosato G: Target-induced death by apoptosis in human lymphokine-activated natural killer cells. Blood 87:2411, 1996

30. Spengler D, Waeber C, Pantaloni C, Holsboer F, Bockaert J, Seeburg PH, Journot L: Differential signal transduction by five splice variants of the PACAP receptor. Nature 365:170, 1993